

Magnesium Acetate Induces a Conformational Change in *Escherichia coli* Primase<sup>†</sup>

Teresa M. Urlacher and Mark A. Griep\*

Department of Chemistry, University of Nebraska—Lincoln, Lincoln, Nebraska 68588-0304

Received July 5, 1995; Revised Manuscript Received September 29, 1995\*

**ABSTRACT:** Primase from *Escherichia coli* is a single-stranded DNA-dependent RNA polymerase. As such, it requires magnesium to carry out catalysis. Limited tryptic digestion was used to probe the conformations of primase as a function of magnesium acetate concentration. In the absence of magnesium, trypsin cleaved primase at three sites. Magnesium acetate induced a conformational change such that one of these sites became inaccessible to trypsin digestion and a new site became trypsin accessible. The conformational change was only induced by  $\text{Mg}(\text{OAc})_2$  and not  $\text{MnCl}_2$ ,  $\text{CaCl}_2$ ,  $\text{NaOAc}$  or  $\text{LiCl}$ , indicating a clear magnesium acetate-dependent conformational change. The effect was slightly induced by  $\text{MgSO}_4$  and  $\text{MgCl}_2$ . An allosteric binding model indicates that primase binds at least two magnesiums in a cooperative manner. The data were best fit to a two-state model in which one conformation had a high affinity for magnesium,  $K_R = 83.4 \text{ M}^{-1}$ , and the other state had virtually no affinity.

*Escherichia coli* primase is a single-strand DNA-dependent RNA polymerase (Swart & Griep, 1993). Its biological function is to synthesize primer RNA during DNA replication (McMacken et al., 1987; Kornberg & Baker, 1992; Marians, 1992). The minimum number of cofactors that primase must interact with to carry out its function at the replication fork include the initiating nucleotide (Kitani et al., 1985), ATP; the second nucleotide, GTP; ssDNA<sup>1</sup> containing the d(CTG) trinucleotide putative recognition sequence (Yoda & Okazaki, 1991); magnesium; zinc (Stamford et al., 1992); DnaB helicase (Zechner et al., 1992a); and DNA polymerase III holoenzyme. Primase has been shown to specifically initiate primer synthesis complementary to the thymidine of the trinucleotide d(CTG) initiation site (Yoda & Okazaki, 1991; Swart & Griep, 1993).

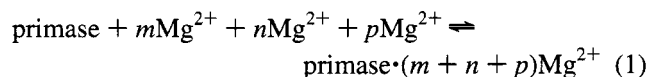
Primase has a zinc prosthetic group (Stamford et al., 1992) but the exact role of zinc in primer synthesis is unclear. Amino acid sequence analysis indicates that both bacterial and bacteriophage primases have eight homologous motifs (Ilyina et al., 1992; Versalovic & Lupski, 1993). Primase contains the putative zinc binding motif Cys-X-X-His-X<sub>17</sub>-Cys-X-X-Cys (CHCC motif) in its amino terminus. In bacteriophage T7 primase the zinc finger has been proposed to be involved in trinucleotide specificity (Bernstein & Richardson, 1988) and may very well be the same for *E. coli* primase. Another possibility is that zinc binds the initiating ATP nucleotide as it does in *E. coli* RNA polymerase (Chatterji & Wu, 1982; Chatterji et al., 1984).

The function of DnaB helicase is to unwind duplex DNA to create the ssDNA that is acted upon by replication proteins. This hexameric protein travels along the lagging strand in a 5' → 3' direction (LeBowitz & McMacken, 1986) driven by its ssDNA-dependent ATPase activity. The carboxyl ter-

minus of primase interacts with DnaB helicase (Tougu et al., 1994). Primase also requires DNA polymerase III holoenzyme to complete replication. This replicative polymerase elongates previously synthesized RNA primers to create 1500-nucleotide Okazaki fragments (Wu et al., 1992; Zechner et al., 1992b).

Magnesium is an important cofactor for DNA and RNA polymerases (Rowen & Kornberg, 1978a; Fairfield et al., 1983; Griep & McHenry, 1989; Kornberg & Baker, 1992; Suh et al., 1992, 1993). Magnesium plays several roles in the function of nucleic acid polymerases including (Black et al., 1994) (1) to bind and neutralize NTP charge [the  $\text{MgATP}^{2-}$  complex has a reported  $K_D$  of 50  $\mu\text{M}$  (Dawson et al., 1986); this allows it to bind to proteins more reversibly]; (2) to bind the  $\beta$ - and  $\gamma$ -phosphates of NTP, making pyrophosphate a better leaving group during phosphodiester bond formation (Burgers & Eckstein, 1979; Joyce & Steitz, 1994); (3) to bind ssDNA as a result of the linear distribution of dense negative charge (Record et al., 1978); (4) to bind protein at sites intended for NTP—magnesium and at sites of local negative charge; (5) to release or bind to ssDNA and protein upon protein/DNA complex formation or dissociation; and (6) to release or bind to ssDNA and protein during protein migration along the DNA (Berg et al., 1981).

One way to summarize the magnesium cations which bind to free primase is



where  $m$  is the number of magnesiums involved in catalysis,  $n$  is the number of magnesiums involved in the conformational change, and  $p$  is the number of nonspecifically bound magnesiums. The values of  $m$ ,  $n$ , and  $p$  may be interdependent. The catalytic magnesium binds the strongest of the three types with typical  $K_{50\% \text{ stimulating}}$  in the range of 5 mM (Swart and Griep, unpublished results).

Amino acid analysis indicates that primase contains at least three sites for magnesium binding (Ilyina et al., 1992; Griep, 1995). One of these magnesium sites closely resembles that

<sup>†</sup> This work was supported in part by NIH Grant GM 47490 to M.A.G. and by a Patricia Roberts Harris Fellowship to T.M.U.

\* Author to whom correspondence should be addressed. Telephone: (402) 472-3429. Telefax: (402) 472-9402. Email: mgriep@unlinfo.unl.edu.

© Abstract published in *Advance ACS Abstracts*, December 1, 1995.

<sup>1</sup> Abbreviations: ssDNA, single-stranded DNA; NTP, ribonucleoside triphosphate; HEPES, *N*-(2-hydroxyethyl)piperazine-*N'*-2-ethanesulfonic acid; SDS, sodium dodecyl sulfate; PVDF, poly(vinylidene difluoride).

of the active magnesium site found in all polymerases (Argos, 1988; Delarue et al., 1990; Joyce & Steitz, 1994) with its conserved aspartates. Site-directed mutagenesis of the "active magnesium" site in DNA polymerase  $\alpha$  showed the largest effect of DNA synthesis when the aspartate was replaced by an asparagine (Copeland & Wang, 1993). This proves the important functional role of this type of magnesium site which binds one of the most critical magnesiums.

Our study focuses on the  $n$  magnesium cations that cause a conformation change. To study primase conformations, we chose limited proteolysis as a sensitive technique (Pedigo & Shea, 1995). At very low protease to protein ratios, the accessibility of residues within the native primase tertiary structure is measured. Regions of proteolytic susceptibility denote surface-exposed regions. Even though trypsin cleaves peptide bonds on the carboxyl site of lysine and arginine residues, under nondenaturing conditions, the tertiary structure of a protein plays a large role as to where cutting occurs. Open or accessible regions of a protein will be digested first. Therefore, limited proteolytic studies such as these can yield important information about changes in the tertiary structure. Previous proteolytic studies of primase indicated that the first site of cleavage is near residue 425 to create 49- and 16.6-kDa peptides (Sun et al., 1994; Tougu et al., 1994). Since these studies used two different proteases, the proteolytic accessibility of this region reflects a unique protein feature rather than a protease feature. Subsequent tryptic cleavage of the 49-kDa fragment results in a 36-kDa peptide which is in turn cleaved to give 13-, 12-, and 11-kDa fragments. While using this method to study primase conformation as a function of salt concentration, we noted a dramatic change in the proteolytic pattern induced by magnesium acetate.

## EXPERIMENTAL PROCEDURES

**Proteins and Enzymes.** Trypsin from bovine pancreas and  $N^\alpha$ -benzoyl-L-arginine *p*-nitroanilide (L-BAPA) were purchased from Sigma. Trypsin concentration was determined spectroscopically using its extinction coefficient of  $14\,400\text{ M}^{-1}\text{ cm}^{-1}$  at 280 nm (Davies & Neurath, 1955). The concentrations of L-BAPA and *p*-nitroaniline also were determined spectroscopically using the extinction coefficients of  $13\,000\text{ M}^{-1}\text{ cm}^{-1}$  at 315 nm and  $8800\text{ M}^{-1}\text{ cm}^{-1}$  at 410 nm, respectively (Erlanger et al., 1961). Primase was isolated from a primase overproducer manufactured by Dr. Roger McMacken's laboratory (Johns Hopkins University, Baltimore, MD) as described previously (Swart & Griep, 1993). The only change was that purification was completed with a 40 mL Q-Sepharose (Pharmacia) ion-exchange column instead of a FPLC MonoQ column.

**Limited Trypsinolysis of Primase.** A typical 25  $\mu\text{L}$  reaction contained 3.0  $\mu\text{M}$  primase and 320 nM trypsin (9.4:1 primase:trypsin) in 50 mM HEPES, pH 7.5, buffer plus salts as indicated. Primase was always preincubated for at least 2 min in the salt solution before trypsin was added to initiate digestion for 15 min at 30 °C. Previous trypsin titrations of primase, performed in the absence of salt, determined the amounts of trypsin needed for the desired cutting pattern. The reactions were quenched with 125 mM Tris, pH 6.8, 4% SDS, 20% glycerol, 10 mM dithiothreitol, and 0.002% bromophenol blue and denatured for 10 min at 95 °C. All samples were centrifuged in a MC 200 NanoFuge (Hoefer Scientific Instruments) before and after each heating period to ensure digestion and recovery of the entire sample.

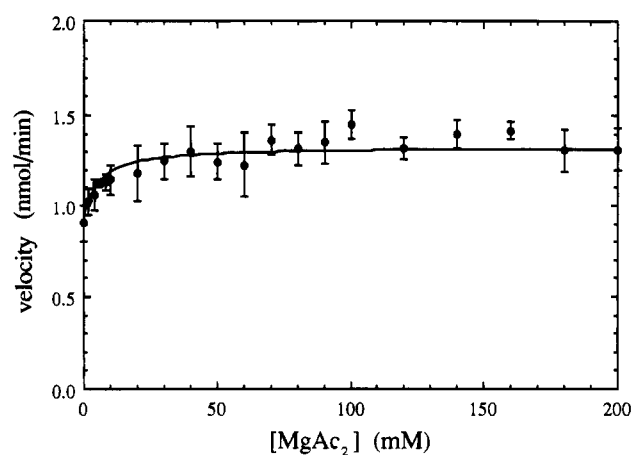


FIGURE 1: Trypsin activity in the presence of magnesium acetate. L-BAPA (1 mM) was digested with trypsin (1.1  $\mu\text{M}$ ) at 30 °C for 15 min as a function of magnesium acetate concentration. The production of *p*-nitroaniline was monitored spectroscopically as described in Experimental Procedures. The error bars at each velocity represent the standard deviation from at least three separate experiments. The data were fit with the equation  $\text{velocity} = 0.90\text{ nmol/min} + \{(0.42\text{ nmol/min})[\text{Mg}(\text{OAc})_2]/(5.0\text{ mM} + [\text{Mg}(\text{OAc})_2])\}$ .

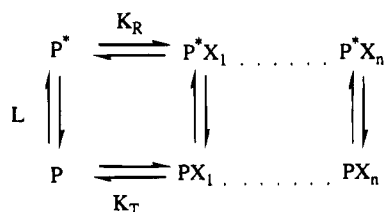
Samples were then applied to a 10–17% SDS–polyacrylamide sucrose gradient gel with a 5% stacking gel (Hames, 1990; Rickwood et al., 1990) which had been prepared using premixed 30% (w/v) 37.5:1 acrylamide:bis(acrylamide) (Bio-Rad). The gradient gel was cast using a SG 500 gradient maker (Hoefer). Electrophoresis was at 30 mA for 2.5 h using the 600SE vertical slab gel unit (Hoefer) and the electrophoresis buffer was 25 mM Tris, pH 7.2, 192 mM glycine, and 0.1% SDS. The protein fragments were visualized by staining with Coomassie Brilliant Blue G Colloidal (Sigma) according to manufacturer's instructions. Molecular mass standards were as follows (Boehringer Mannheim): fructose-6-phosphate kinase, 85 204 Da; glutamate dehydrogenase, 55 562 Da; aldolase, 39 212 Da; triose phosphate isomerase, 26 626 Da; trypsin inhibitor, 20 100 Da; and lysozyme, 14 307 Da.

**Quantitation of Band Intensity for Limited Tryptic Digestion.** The stained SDS–polyacrylamide gels were scanned with a Hewlett-Packard Scan Jet IICx/T set to 200 dpi. The image was then quantified by ImageQuant software from Molecular Dynamics by integrating the volume of each band to give absolute intensities of the tryptic bands.

**Determination of Trypsin Activity.** The chromogenic substrate, L-BAPA, release *p*-nitroaniline, a yellow product, upon trypsin digestion which was analyzed spectroscopically (Erlanger et al., 1961). Control experiments established the amounts of L-BAPA and trypsin to use in the assay. The determination of trypsin activity was done in the presence and absence of magnesium acetate to determine the effect of this salt. Reactions of 400  $\mu\text{L}$  contained 1 mM L-BAPA, 1.1  $\mu\text{M}$  trypsin, and 50 mM HEPES, pH 7.5, plus magnesium acetate. Reaction tubes were incubated for 2 min at 30 °C prior to initiating with trypsin. Reactions were then quenched with 100  $\mu\text{L}$  of 30% acetic acid after incubation for 15 min at 30 °C. Absorbance readings at 410 nm determined the nanomoles of *p*-nitroaniline produced which was proportional to the nanomoles of active trypsin. Analysis showed that trypsin was stimulated 45% at  $\text{Mg}(\text{OAc})_2$  concentrations of 10 mM (Figure 1). The  $K_{50\%}$  was 5 mM  $\text{Mg}(\text{OAc})_2$ , which was an important consideration in analyzing the primase tryptic data. This observation did not hinder analysis of

primase trypsinolysis data; it only increased the awareness of trypsin salt sensitivity.

**Theoretical Calculations.** In the simplest model there were two conformations of primase, a taut form, P, and a relaxed form, P\*, in a state of equilibrium. Either form can bind the magnesium cations. In addition, there may be magnesiums bound to primase that are not involved in the conformational change. However, we only measured the number of magnesiums that promoted structural changes due to interactions with specific amino acid residues. The binding of magnesium ions to primase can be represented by the allosteric binding model



and the experimental data fit to the equation (Cantor & Schimmel, 1980)

$$\phi = \frac{(1 + K_R X)^n}{(1 + K_R X)^n + L(1 + K_T X)^n} \quad (2)$$

where  $L$  is the equilibrium ratio of the taut form to the relaxed form;  $K_R$  is the equilibrium ratio of relaxed form binding the first magnesium to the free relaxed form;  $K_T$  is the equilibrium ratio of the taut form binding the first magnesium to the free taut form;  $X$  is the ligand, in this case magnesium;  $n$  is the number of magnesium cations involved in the conformational change; and  $PX_n$  and  $P^*X_n$  are the taut or relaxed forms, respectively, bound to  $n$  magnesium. The value of  $L$  can be experimentally determined from the fraction of primase that is in the highest bound relaxed state to the least bound taut state. The value of  $L$  was 18 as determined from the mean of all titrations.  $K_T$  and  $K_R$  were the values obtained from fits of the overall averaged data set ( $[Mg(OAc)_2]$ ,  $\phi_{obsd}$ ) to eq 2 when  $n$  was set to 2, 3, or 4. From the best fit,  $\phi_{calcd}$  was obtained and compared to  $\phi_{obsd}$  to determine the standard deviation,  $\sigma$  fit.  $\sigma$  fit was the standard deviation for the entire data set between  $\phi_{calcd}$  and  $\phi_{obsd}$ .

**Primase Fragment Activity.** The activities of primase and primase tryptically digested in the presence or absence of 100 mM  $Mg(OAc)_2$  were determined after separating reactions by gel filtration. Each 500  $\mu$ L reaction in 50 mM HEPES, pH 7.5, buffer contained 3.0  $\mu$ M primase with two reactions containing 100 nM trypsin. The reactions were incubated at 30 °C for 15 min and then applied to a 10 mL Sephacryl S-200 (Pharmacia) gel filtration column. Fractions (390  $\mu$ L) were collected using a FC-80K fractionator (Gilson) and eluted with 1.5 column volumes of 50 mM HEPES, pH 7.5, 100 mM potassium glutamate, and 10 mM dithiothreitol buffer. Protein was identified in the resulting fractions by measuring the absorbance at 280 nm. Activity was determined by the M13Gori assay for primase described previously (Griep & McHenry, 1989). One unit of primase was defined as the amount needed to incorporate 1 pmol of total nucleotide/min into acid-precipitable DNA at 30 °C in 5 min under conditions where all other components were saturating.

To determine the peptide content of each fraction, a SDS-polyacrylamide gel was run. Only fractions throughout the activity peak were analyzed on the gel. Denaturing buffer was added to 50  $\mu$ L of each fraction, and the fraction was denatured by heating for 10 min at 95 °C. Samples were then applied to a 10–17% SDS-polyacrylamide sucrose gradient gel with a 5% stacking gel. The samples were electrophoresed and the gel was stained as described above.

**Sequence Determination of Tryptic Peptides.** A 10–17% SDS-polyacrylamide sucrose gradient gel was run as described above. Primase tryptic peptides were electroeluted to Westran (Schleicher & Schuell), a PVDF membrane, in a 20 mM Tris, pH 8.0, 192 mM glycine, 20% methanol, and 0.1% SDS transfer buffer. The electroelution was performed for 15 h at 30 V. The PVDF membrane was thoroughly rinsed with deionized water, stained with Coomassie Brilliant Blue G Colloidal (Sigma), and destained with 50% methanol/10% acetic acid. Specific peptide bands were cut out of the stained PVDF membrane and subjected to automated peptide sequencing on an applied Biosystems Procise 491 sequencer with an on-line 140C analyzer (Protein Structure Core Facility, University of Nebraska Medical Center, Omaha, NE). Peptide sequences were matched to primase using the GCG program (Program Manual for the Wisconsin Package, Version 8, September 1994, Genetics Computer Group, Madison, WI). The masses for each tryptic peptide were calculated using the GCG peptidesort program. The peptide masses referred to in the text are the apparent SDS-PAGE mass and not the calculated mass.

## RESULTS

Little is known about primase conformations. Thus, we undertook a study of the effect of various primase cofactors on the tryptic susceptibility of primase. In the presence of  $Mg(OAc)_2$ , the tryptic banding pattern revealed dramatic conformational changes in the primase tertiary structure.

**Tryptic Titration of Primase.** During a 15-min incubation, nearly every single-chain primase (3.0  $\mu$ M) was cleaved at least once in the presence of 320 nM trypsin (Figure 2A). Between 24 and 192 nM trypsin the most tryptically resistant peptides were a 51- and 49-kDa multiplet and smaller singlets of 13.6 and 16.6 kDa. Above 192 nM trypsin, a 37- and 35-kDa doublet was the most tryptically resistant and coincided with a generation of several peptides in the range of 13.6 kDa. Minor products included 63-, 37-, 30-, and 21-kDa peptides. These observations correlate with previous digestion studies (Sun et al., 1994; Tougu et al., 1994).

A significantly different digestion pattern was observed when 100 mM  $Mg(OAc)_2$  was included in the digestion buffer (Figure 2B). At low trypsin concentration (4–24 nM), the digestion pattern was identical to primase digestion without magnesium acetate where the peptide backbone was cleaved three times. However, by 32 nM trypsin faint bands of 42 and 40 kDa were observed. This new 42- and 40-kDa doublet became and remained very apparent as the trypsin concentration was increased. It was also clear that the appearance of the 16.6-kDa peptide was coincidental with the new 42- and 40-kDa doublet.

**Primase Tryptic Sites.** The first tryptic peptide to be generated was 63 kDa and had the amino-terminal sequence LKKQG (Figure 3). This indicated that the first cleavage site was Lys28 and that this residue of primase was well exposed to solvent and trypsin. Efficiency of trypsin

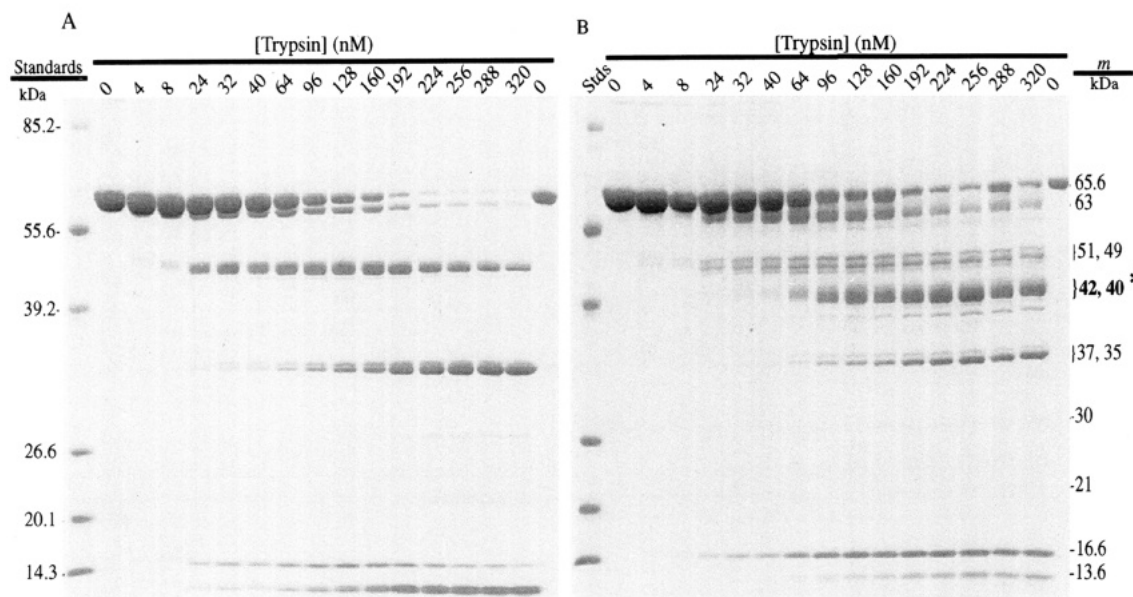


FIGURE 2: Trypsin titration of primase. (A) Primase was digested with trypsin at various trypsin concentrations, and the samples were denatured, electrophoresed on a 10–17% SDS–polyacrylamide gradient gel, and stained with Coomassie Blue. (B) Primase was incubated with 100 mM  $\text{Mg}(\text{OAc})_2$  prior to digestion with various trypsin concentrations, and then the samples were treated as in part A. Reaction conditions were as described under Experimental Procedures. The concentration of trypsin is indicated along the top of the gels. Migration of the molecular mass standards (stds) is shown on the left, and the apparent molecular mass,  $m$ , of the tryptic fragments is shown on the right. Note that the 42- and 40-kDa (\*) peptide is only observed in part B containing 100 mM  $\text{Mg}(\text{OAc})_2$ .

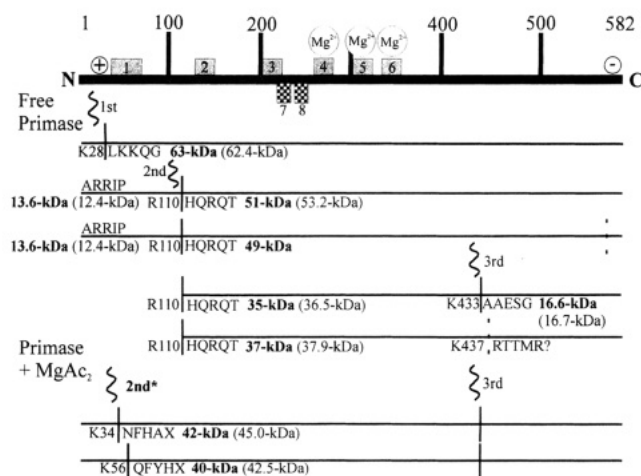


FIGURE 3: Primase digestion map. Primase primary structure contains six conserved motifs (shaded boxes; Ilyina et al., 1992; Versalovic & Lupski, 1993). The functions of some of the motifs have been hypothesized on the basis of their similarities of other protein's motifs. Motif 1 is a "zinc finger" motif which is involved in sequence-specific initiation. Motif 5 is referred to as the "active magnesium" binding site. Motif 7 is highly conserved and represents the RNA polymerase motif. Motif 8 is a signature sequence common to all bacterial primases (Versalovic & Lupski, 1993). The digestion map shows the sequence for the first five amino-terminal residues from each peptide sequenced in the presence and absence of high magnesium acetate concentrations. In the presence of magnesium acetate, the second cleavage site (2nd\*) is shifted. The masses in bold print are the apparent masses from the SDS–PAGE while the calculated masses are indicated in parentheses. The vertical solid lines are the sites at which cleavage was determined to occur, and the dashed lines represent where cleavage is hypothesized to occur.

cleavage at this site was very low, and much full-length primase remained when cleavage began at the second site. The next peptides to be generated were 51 and 49 kDa, and they both had amino-terminal sequences of HQRQT. A 13.6-kDa peptide with sequence of ARRIP was generated simultaneously. This indicated that the second cleavage site was Arg110 and that the 51-kDa peptide was from His111

to the carboxyl terminus. In contrast, the 49-kDa peptide must have been formed from additional inefficient cleavage near the carboxyl terminus (Figure 3, dashed vertical line). The 13.6-kDa peptide had a sequence that differs in one amino acid from wild-type primase in that the third position was an arginine and not a glycine (Burton et al., 1983). The third cleavage site was at Lys433, generating a 37- and 35-kDa doublet along with a 16.6-kDa peptide. The 35- and 37-kDa peptides both had the amino-terminal sequence of HQRQT, and the 16.6-kDa sequence was AAESG. The 35-kDa peptide was consistent with having the sequence from His111 to Lys433. We hypothesize that the 37-kDa peptide had the sequence from His111 to Lys437 even though the corresponding carboxyl-terminal peptide Arg438 to Lys582 terminus was not observed. Generation of the 30- and 21-kDa peptides is from subsequent digestion of the 51- and 49-kDa multiplet and the 37- and 35-kDa doublet. These minor products were not sequenced due to low yield in the tryptic digestions.

The second most accessible cleavage site was sensitive to magnesium acetate. In the presence of magnesium, the second fastest cleavage no longer occurred at Arg110 but at Lys34 and Lys56 to generate a peptide doublet at 42 and 40 kDa, respectively. The 42-kDa band had an amino-terminal sequence of NFHAX and the 40-kDa band had a sequence of QFYHX. In both peptides, the unidentified X residue correlated to cysteine residues in the primase sequence (Burton et al., 1983).

Previous trypsinolysis studies of primase (Tougu et al., 1994) agree in most respects with our digestion analysis. However, compared to their longest incubation time, we observed more peptide cutting on average. From our data, we can estimate that each single chain of primase was cleaved at least three times total. The major difference is that we observe a multiplet including 51 (His111–Lys582) and 49 kDa (His111–?) whereas they observed a singlet of 49 kDa (Ala2–Lys433). It is possible that their 49 kDa (Ala2–Lys433) was among the peptides in our multiplet but

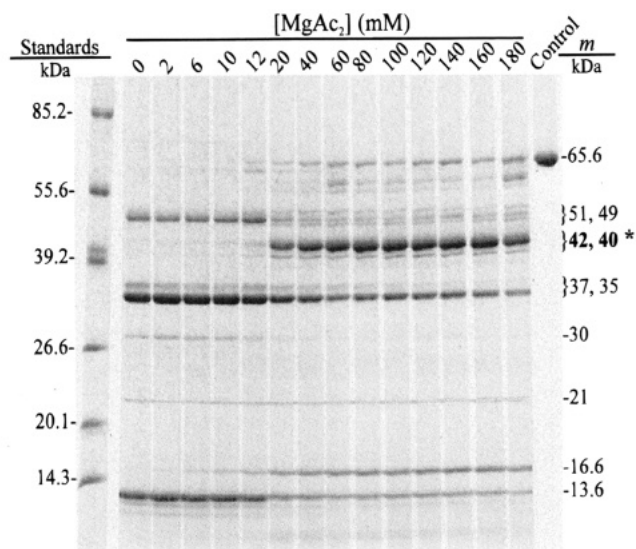


FIGURE 4: Magnesium acetate titration of primase. Primase was digested by trypsin in the presence of various magnesium acetate concentrations as indicated along the top of the gel. Reaction conditions are described under Experimental Procedures. Migration of the molecular mass standards is shown on the left, and the apparent SDS-PAGE molecular mass,  $m$ , of the tryptic fragments is shown on the right. Note the appearance of the 42- and 40-kDa (\*) doublet as the concentration of  $\text{Mg}(\text{OAc})_2$  was increased.

that its sequence was not observed. These differences in our multiplet and their singlet must be due to different buffer conditions.

**Magnesium-Induced Primase Structural Changes.** Determination of the amount of magnesium required to induce the conformational change required tryptic digestion in the presence of magnesium acetate (Figure 4). The determination was performed at a high trypsin concentration of 320 nM because the effect was observed most clearly at the higher trypsin to primase ratios. The studies of Ackers and co-workers (Brenowitz et al., 1986) on DNA-protein footprinting thermodynamics have also found that even though "single-hit" kinetics are desirable theoretically (only 15% of the backbones cleaved once), a stronger signal change achieved with greater backbone cutting does not significantly perturb the data analysis. Even though the change could be monitored at low trypsin to primase ratios, the signal change was smaller and more difficult to measure. At  $\text{Mg}(\text{OAc})_2$  concentrations less than 6 mM, all single-chain primase (3.0  $\mu\text{M}$ ) was cleaved at least once by trypsin (320 nM) (Figure 4). The prominent peptides generated were the 51- and 49-kDa multiplet, the 37- and 35-kDa doublet, and several singlets shorter than 13.6 kDa. More full-length primase was observed as the  $\text{Mg}(\text{OAc})_2$  concentration was increased. This indicated that  $\text{Mg}(\text{OAc})_2$  protected primase from trypsin digestion. The trypsin activity assay using L-BAPA, a chromogenic substrate, determined that, at the magnesium concentration required for the primase conformational change, trypsin cleaved 45% more peptide bonds than in the absence of magnesium. Even though trypsin now cleaved three sites for every two that were cleaved in the absence of magnesium (Figure 1), primase was cleaved less (Figure 4), indicating even more protection than what was observed.

Another significant change was observed in the 37- and 35-kDa doublet (Figure 4). The appearance of the 42- and 40-kDa doublet coincided with the disappearance of the 51- and 49-kDa multiplet and part of the 37- and 35-kDa doublet. A plot of the fraction of 42- and 40-kDa peptides compared

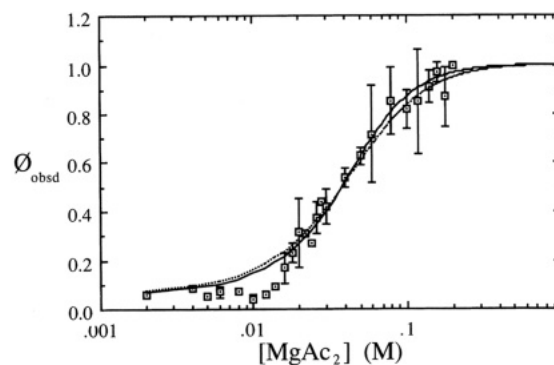


FIGURE 5: Effect of magnesium acetate on primase conformation. The fractional intensity of the 42- and 40-kDa doublet,  $\phi_{\text{obsd}}$ , was measured at each magnesium concentration. The values from ( $n = 2$ , dashed line;  $n = 3$ , straight line) Table 1 were used in eq 2 to generate the fit data. The error bars at each  $\phi_{\text{obsd}}$  represent the standard deviation from at least four separate determinations. The data with the five largest standard deviations (20, 60, 80, 120, and 180 mM) each have a single value that is more than one standard deviation unit away from the mean.

to the fraction of the 37- and 35-kDa peptides as a function of  $\text{Mg}(\text{OAc})_2$  showed that the appearance of the 42- and 40-kDa bands correlated to the disappearance of the 37- and 35-kDa bands (data not shown). The crossover point,  $K_{50\%}$ , was 40 mM. As the  $\text{Mg}(\text{OAc})_2$  concentration was increased, the most stable peptides became 42 kDa and 40 kDa. These peptides were only induced by  $\text{Mg}(\text{OAc})_2$  and not  $\text{MnCl}_2$ ,  $\text{CaCl}_2$ ,  $\text{NaOAc}$ , or  $\text{LiCl}$ , indicating a clear magnesium acetate-dependent conformational change. The effect was slightly induced by  $\text{MgSO}_4$  and  $\text{MgCl}_2$ . The exact role of the acetate ion was unclear, but the monovalent anion could interact strongly with positive regions of the primase molecule, allowing for unraveling of the sequences flanking the core structure. It was clear that the acetate ion had much more of an effect than either the sulfate or chloride ions. This was not a simple ionic strength effect because sodium acetate does not induce the change. This left the responsibility for the conformational change on the cation, in this case magnesium.

**Magnesium-Primase Binding Affinity.** The intensity of the 42- and 40-kDa doublet at each magnesium concentration was taken to represent the extent of primase conformational change. Quantitation of the fraction of primase that had undergone the conformational change,  $\phi_{\text{obsd}}$ , involved calculating the ratio of the doublet to the most intense titration point. Visual inspection of the magnesium-induced primase conformational change indicated that  $K_{50\%}$  was about 40 mM (Figure 5). A Hill plot revealed a Hill coefficient of 1.8 when two binding sites were assumed, indicating strong cooperativity. Likewise, a Scatchard plot was concave, indicating a positively cooperative system. Therefore, the magnesium conformational change involved at least two magnesiums and was positively cooperative. To obtain a better description of the magnesium-induced conformational change, we fit the data to a two-state model. In the taut state, primase binds magnesium more weakly than in the relaxed state. The model does not assume the order in which the states bind the magnesium.

Comparison of the experimental data to the fit data revealed a very good correlation at most  $\text{Mg}(\text{OAc})_2$  concentrations (Figure 5). The number of magnesiums involved in the conformational change could not be determined conclusively because the model does not fail even at a very



Table 1: Allosteric Model Parameters for Primase Binding to Magnesium Acetate<sup>a</sup>

<i>n</i>	$K_T$ ( $M^{-1}$ )	$K_R$ ( $M^{-1}$ )	$\sigma$ fit
2	0 <sup>b</sup>	83.4	0.0563
3	1.52	46.0	0.0497
4	3.97	35.9	0.0486

<sup>a</sup> In the allosteric model, *n* is the number of total magnesium binding sites,  $K_T$  is the affinity of the taut form of primase for magnesium,  $K_R$  is the affinity of the relaxed form of primase for magnesium, and  $\sigma$  fit is the standard deviation between  $\phi_{\text{calcd}}$  and  $\phi_{\text{obsd}}$  for the entire data set.

<sup>b</sup> Fit value was actually  $10^{-17}$  but can be considered zero.

high number of magnesium cations. For example,  $\sigma$  fit was relatively unchanged when  $n = 12$  was compared to the  $\sigma$  fit for two, three, and four magnesiums. In the simplest model where  $n = 2$ , the model indicated that only the relaxed form of primase bound magnesium;  $K_T$  was zero (Table 1). When  $n = 3$  or 4, the  $K_T$  values are larger and closer to the  $K_R$  values. The most noticeable deviation between the experimental and fit data occurred in the range of 8–16 mM  $Mg(OAc)_2$  (Figure 5). This interesting anomaly suggested possible negative cooperativity of primase in the taut form before the conformational change to the relaxed form. A better fit at low  $Mg(OAc)_2$  concentration might be found by including a negative cooperativity parameter, but it would be expected then that the fit at high  $Mg(OAc)_2$  concentration would be deviating. Clearly, more work in this narrow range needs to be done to better describe its origin, but it may be related to the binding of the “active magnesium”. As expected from this model,  $K_R$  was always larger than  $K_T$ , indicating that primase prefers to bind magnesium in the relaxed conformation, thus supporting positive cooperative behavior. Therefore, the magnesium-induced conformational change was caused by at least two magnesium cations.

**Activity of Tryptically Digested Primase.** To determine whether the conformational change in primase affected the activity, we isolated digested and undigested primase by gel filtration and assayed their activity in the M13Gori assay (Griep & McHenry, 1989). This assay is a coupled RNA/DNA synthesis assay requiring primase to synthesis a RNA primer that can be elongated by DNA polymerase III holoenzyme. Primase, in three separate reactions of untreated, trypsin digested, and trypsin digested in the presence of 100 mM  $Mg(OAc)_2$ , eluted from the gel filtration column at the same location (Figure 6). This indicated that even though primase had been digested, its fragments do not readily dissociate under nondenaturing conditions. However, the activity of these three different reactions was not identical. Fraction 18 of the untreated primase was a single-chain peptide of 65.6 kDa when resolved on a 10–17% SDS–polyacrylamide sucrose gradient gel and had an activity of 21 units/ $\mu$ L. Primase digested with trypsin showed no single-chain remained and was four times less active than undigested primase. Two major peptide products were generated, a 49- and 51-kDa multiplet and a 37- and 35-kDa doublet. Primase digested in the presence of 100 mM  $Mg(OAc)_2$  was 10-fold less active than the reaction containing undigested primase. This treated primase did not result in a 49- and 51-kDa multiplet but instead consisted of 42- and 40-kDa peptides and some of the 35-kDa peptide. These data indicated that the high  $Mg^{2+}$  conformation was less active than the low  $Mg^{2+}$  conformation.

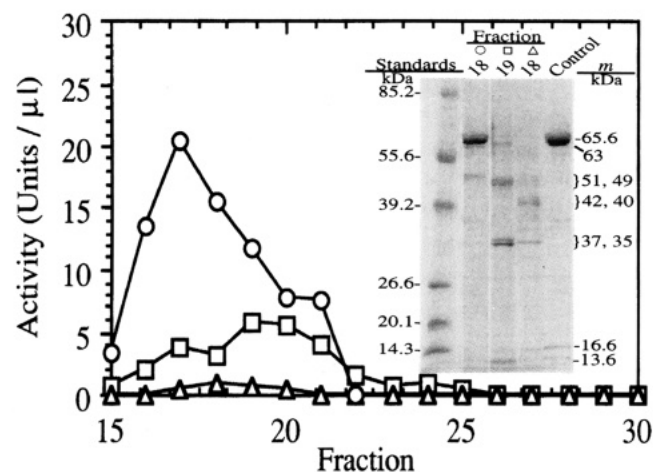


FIGURE 6: Activity of primase conformations. Primase (3.0  $\mu$ M) was incubated for 15 min at 30 °C alone ( $\circ$ ), with 100 nM trypsin ( $\square$ ), or with 100 nM trypsin and 100 mM  $Mg(OAc)_2$  ( $\triangle$ ) and then applied to a gel filtration column. Activity was determined for each eluting fraction, and 10–17% SDS–polyacrylamide gradient gel was electrophoresed according to conditions under Experimental Procedures. Only the peak activity fractions are shown in the inset. Migration of the molecular mass standards is shown on the left, and the apparent molecular mass, *m*, of the peptide fragments is shown on the right.

## DISCUSSION

Before primase actually synthesizes the oligoribonucleotide on the single-stranded DNA template, a set of interactions must take place. One of these interactions includes binding of magnesium. The ability of nucleic acid polymerases to bind magnesium has not received much attention because of the difficulty of measuring this interaction. We show here that primase undergoes a dramatic change in conformation that is possible to measure. Magnesium binds to at least two sites on primase to cause a large conformational change.

Even though the conformational change is dramatic, the possible interdependence of the *m* catalytic magnesium, *n* conformational change magnesium, and *p* nonspecific magnesium (eq 1) makes it difficult to study each type of magnesium separately. Work in our laboratory shows that primase requires magnesium for activity and that activity is stimulated from 0 to 10 mM (Swart and Griep, unpublished results). The *m* catalytic magnesium probably binds to the “active magnesium” site at motif 5 (Figure 3) and may involve one or two magnesium ions. The active magnesium site is a conserved feature of all polymerases (Mildvan & Loeb, 1979; Argos, 1988; Delarue et al., 1990; Ilyina et al., 1992) and appears to involve two, possibly three, regions of primase. The observation that at least two magnesiums are involved in the conformational change of primase leads to several hypotheses: (1) the second magnesium may displace one of the portions of primase that had been bound to the active magnesium, or (2) there could be two regions of primase distinct from the active magnesium site involved only in the conformational change. In the latter case, the allosteric conformations may represent forms involved in the regulation of primer initiation or elongation.

The allosteric model of magnesium binding to primase is in good agreement with the data (Figure 5) except below 10 mM  $Mg(OAc)_2$ . This interesting observation leads to speculation about primase cooperativity. It is possible that primase’s affinity for the initial conformational change magnesium ion is low, yielding anticooperative behavior (i.e., deviation from the model). Thus, only after primase has

bound one magnesium does positive cooperativity dominate and then primase binding behavior complies with the two-state model in which the taut form is active and the relaxed form much less active.

There are two possible explanations for this conformational response of primase to magnesium, either metal concentration control of cellular DNA replication or involvement in the primer elongation step. An elongation kinetics model determined by Johnson and co-workers for T7 DNA polymerase (Patel et al., 1991) involves a rate-limiting conformational change that occurs after incorporation of a NTP. Their conformational change is likely to be coincident with polymerase translocation from the terminal phosphodiester bond to the bound NTP. Perhaps the two conformations that we have identified are similar to these two conformations involved in the translocation. In which case, magnesium is necessary in the translocation step of primer elongation. The translocation step would involve an inactive, relaxed form of primase moving on the primer/template complex to the next available template site. Once at the new site, the conformation changes back to the active, taut form, necessary for the incorporation of the NTP.

There are two possibilities as to how magnesium binding to primase alters its tryptic sensitivity. Besides the conserved and closely spaced acidic residues in motifs 4, 5, and 6 there is a cluster of acidic residues between residues 81 and 100 high in glutamate content to which magnesium ions could bind. Perhaps magnesium binding at this site prevents cleavage at the adjacent Arg110 resulting in decreased cleavage by trypsin. If the conformation did not also change, then a simple increase in cleavage at all other sites would be observed. This is not observed, however. Instead, the second cleavage site shifts to either Lys34 or Lys56 to create the 42- and 40-kDa doublet. These sites are at motif 1, the "zinc finger" (Ilyina et al., 1992). The 40-kDa fragment is formed by cleavage within the zinc finger motif and is always less intense than the 42-kDa band, suggesting that this occurs only after the cleavage at Lys34.

Future work in this area will define the preinitiation and elongation binding complexes. Competing effects of magnesium and nucleotide substrates with primase are currently being investigated along with a possible second zinc interaction.

## ACKNOWLEDGMENT

We thank Teresa Rush for isolation and purification of *E. coli* primase. We especially thank Dr. Lawrence J. Parkhurst for help with computer modeling of primase-magnesium binding.

## REFERENCES

- Argos, P. (1988) *Nucleic Acids Res.* 16, 9909–9916.
- Berg, O. G., Winter, R. B., & von Hippel, P. H. (1981) *Biochemistry* 20, 6929–6948.
- Bernstein, J. A., & Richardson, C. C. (1988) *Proc. Natl. Acad. Sci. U.S.A.* 85, 396–400.
- Black, C. B., Huang, H.-W., & Cowan, J. A. (1994) *Coord. Chem. Rev.* 135/136, 165–202.
- Brenowitz, M., Senear, D. F., Shea, M. A., & Ackers, G. K. (1986) *Methods Enzymol.* 130, 132–181.
- Burgers, P. M. J., & Eckstein, F. (1979) *J. Biol. Chem.* 254, 6889–6893.
- Burton, Z. F., Gross, C. A., Watanabe, K. K., & Burgess, R. R. (1983) *Cell* 32, 335–349.
- Cantor, C. R., & Schimmel, P. R. (1980) *Biophysical Chemistry*, Part III, W. H. Freeman and Co., New York.
- Chatterji, D., & Wu, F. Y.-H. (1982) *Biochemistry* 21, 4657–4664.
- Chatterji, D., Wu, C. W., & Wu, F. Y.-H. (1984) *J. Biol. Chem.* 259, 284–289.
- Copeland, W. C., & Wang, T. S.-F. (1993) *J. Biol. Chem.* 268, 11028–11040.
- Davies, E. W., & Neurath, H. (1955) *J. Biol. Chem.* 212, 515.
- Dawson, R. M. C., Elliott, D. C., Elliott, W. H., & Jones, K. M. (1986) *Data for Biochemical Research*, 3rd ed., Oxford University Press, New York.
- Delarue, M., Poch, O., Tordo, N., Moras, D., & Argos, P. (1990) *Protein Eng.* 3, 461–467.
- Erlanger, B. F., Kokowsky, N., & Cohen, W. (1961) *Arch. Biochem. Biophys.* 95, 271–278.
- Fairfield, F. A., Newport, J. W., Dolejsi, M. K., & von Hippel, P. H. (1983) *J. Biomol. Struct. Dyn.* 1, 715–727.
- Griep, M. A. (1995) *Indian J. Biochem. Biophys.* 32, 171–178.
- Griep, M. A., & McHenry, C. S. (1989) *J. Biol. Chem.* 264, 11294–11301.
- Hames, B. D. (1990) in *Gel Electrophoresis of Proteins: A Practical Approach* (Hames, B. D., & Rickwood, D., Eds.) pp 1–147, IRL Press, Oxford.
- Ilyina, T. V., Gorbalenya, A. E., & Koonin, E. V. (1992) *J. Mol. Evol.* 34, 351–357.
- Joyce, C. M., & Steitz, T. A. (1994) *Annu. Rev. Biochem.* 63, 777–822.
- Kitani, T., Yoda, K.-y., Ogawa, T., & Okazaki, T. (1985) *J. Mol. Biol.* 184, 45–52.
- Kornberg, A., & Baker, T. A. (1992) *DNA Replication*, 2nd ed., W. H. Freeman and Co., New York.
- LeBowitz, J. H., & McMacken, R. (1986) *J. Biol. Chem.* 261, 4738–4748.
- Marians, K. J. (1992) *Annu. Rev. Biochem.* 61, 673–719.
- McMacken, R., Silver, L., & Georgopoulos, C. (1987) in *Escherichia coli and Salmonella typhimurium: Cellular and Molecular Biology* (Neidhardt, F. C., Ed.) pp 564–612, American Society for Microbiology, Washington, DC.
- Mildvan, A. S., & Loeb, L. A. (1979) *CRC Crit. Rev. Biochem.* 6, 219–244.
- Patel, S. S., Wong, I., & Johnson, K. A. (1991) *Biochemistry* 30, 511–525.
- Pedigo, S., & Shea, M. A. (1995) *Biochemistry* 34, 1179–1196.
- Record, M. T., Jr., Anderson, C. F., & Lohman, T. M. (1978) *Q. Rev. Biophys.* 11, 103–178.
- Rickwood, D., Chambers, J. A. A., & Spragg, S. P. (1990) in *Gel Electrophoresis of Proteins: A Practical Approach* (Hames, B. D., & Rickwood, D., Eds.) pp 217–272, IRL Press, Oxford.
- Rowen, L., & Kornberg, A. (1978a) *J. Biol. Chem.* 253, 758–764.
- Stamford, N. P. J., Lilley, P. E., & Dixon, N. E. (1992) *Biochim. Biophys. Acta* 1132, 17–25.
- Suh, W. C., Leirmo, S., & Record, M. T., Jr. (1992) *Biochemistry* 31, 7815–7825.
- Suh, W.-C., Ross, W., & Record, M. T. J. (1993) *Science* 259, 358–361.
- Sun, W., Tormo, J., Steitz, T. A., & Godson, G. N. (1994) *Proc. Natl. Acad. Sci. U.S.A.* 91, 11462–11466.
- Swart, J. R., & Griep, M. A. (1993) *J. Biol. Chem.* 268, 12970–12976.
- Tougu, K., Peng, H., & Mariani, K. J. (1994) *J. Biol. Chem.* 269, 4675–4682.
- Versalovic, J., & Lupski, J. R. (1993) *Gene* 136, 281–286.
- Wu, C. A., Zechner, E. L., & Mariani, K. J. (1992) *J. Biol. Chem.* 267, 4030–4044.
- Yoda, K.-y., & Okazaki, T. (1991) *Mol. Gen. Genet.* 227, 1–8.
- Zechner, E. L., Wu, C. A., & Mariani, K. J. (1992a) *J. Biol. Chem.* 267, 4045–4053.
- Zechner, E. L., Wu, C. A., & Mariani, K. J. (1992b) *J. Biol. Chem.* 267, 4054–4063.

BI951495L